Controlling the Shape and Chirality of an Eight-crossing Molecular Knot

John P. Carpenter,‡ Charlie T. McTernan,‡ Jake L. Greenfield, Roy Lavendomme, Tanya K. Ronson and Jonathan R. Nitschke*

[1]Department of Chemistry, University of Cambridge, Lensfield Road, Cambridge, CB2 1EW, UK

‡ these authors contributed equally

*e-mail: jrn34@cam.ac.uk

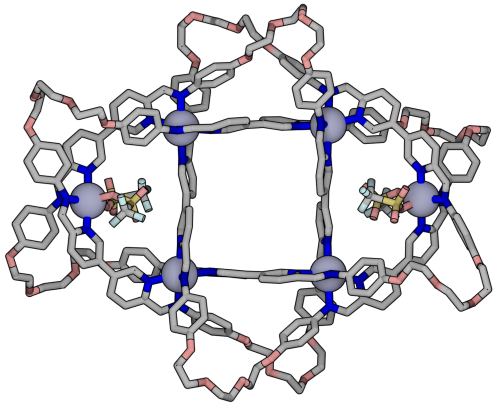

Abstract

The knotting of biomolecules impacts their function, and enables them to carry out new tasks. Likewise, complex topologies underpin the operation of many synthetic molecular machines. The ability to generate and control more complex knotted architectures is essential to endow these machines with more advanced functions. Here we report the synthesis of a molecular knot with eight crossing points, consisting of a single organic loop woven about six templating metal centres, *via* one-pot self-assembly from a simple pair of dialdehyde and diamine subcomponents and a single metal salt. The structure and topology of the knot were established by NMR spectroscopy, mass spectrometry and X-ray crystallography. Upon demetallation, the purely organic strand relaxes into a symmetric conformation, whilst retaining the topology of the original knot. This knot is topologically chiral, and may be synthesised diastereoselectively through the use of an enantiopure diamine building block.

Knots are one of the oldest technologies, having been used for thousands of years to transform the properties of the materials in which they are tied.[1] At the molecular level, knots are found in biology in proteins and DNA,[2,3] and form spontaneously in sufficiently long polymer chains.[4,5] Chain breakage in these polymer systems occurs most readily at the knotted point,[6] whereas knotting together of proteins in the HK97 viral capsid renders it more robust.[7] Knotting at the molecular level thus has major effects upon material properties.[8,9] Since Sauvage's first full characterisation of synthetic knotted molecules three decades ago,[10] the beauty of these woven architectures has attracted chemists,[11] leading to recent breakthroughs in the synthesis of complex, highly symmetric, knots,[12,13,14,15,16,17,18] and to investigations of their functions.[19,20]

To date, synthetic routes to molecular knots and links have focussed on the preparation of highly symmetric knots with few crossing points, such as the three-crossing trefoil knot.[21,22,23,24,25,26,27,28,29,30] Symmetrical higher order knots and links with up to nine crossing points have recently been prepared,[31] often based on the circular helicate approach pioneered by the Leigh group.[32,33] These increasingly complex knots have been used to control catalysis,[19,34] and they show strong and specific anion binding.[35] Many molecular knots are topologically chiral, possessing handedness that arises from the way in which their strands are woven together. Given that chirality is critical to function in nature and technology,[36,37] the control of chirality in topologically complex molecular architectures is anticipated to enable progressively more complex applications.[38,39] Topologically stereoselective synthesis has been achieved for trefoil knots,[40,41] and for knots formed from combinations of trefoil knots,[28,31] but no route to control the topological chirality of higher covalent knots has yet been reported.

Here we report the single-step synthesis of a molecular knot with eight crossing points, an 8_{19} knot.[12] This knot was formed in a single step by the subcomponent self-assembly of a diamine, a dialdehyde, and a metal salt. Upon reduction and demetallation, the knot relaxed into a higher-symmetry configuration. Furthermore, embedding remote stereocentres into the diamine subcomponent enabled control over the topological chirality of the 8_{19} knot product.

Results and discussion

The 8_{19} molecular knot reported herein consists of a single organic molecular strand which weaves a continuous path about six templating metal centres. This entangled molecule can be prepared through either a single-step process, or in stepwise fashion from a pre-assembled grid in enhanced yield.

Subcomponent **A** (Fig. 1) has been shown to self-assemble with *p*-toluidine and different metal salts to produce a family of structurally distinct supramolecular architectures.[42,43,44] One of these is the M_6L_8 (where M = Co^{II}, Ni^{II}, Zn^{II}) extended circular helicate **1** (Fig. 1, Zn-**1**). In **1**, eight bis-bidentate ligands weave about the six metal centres.

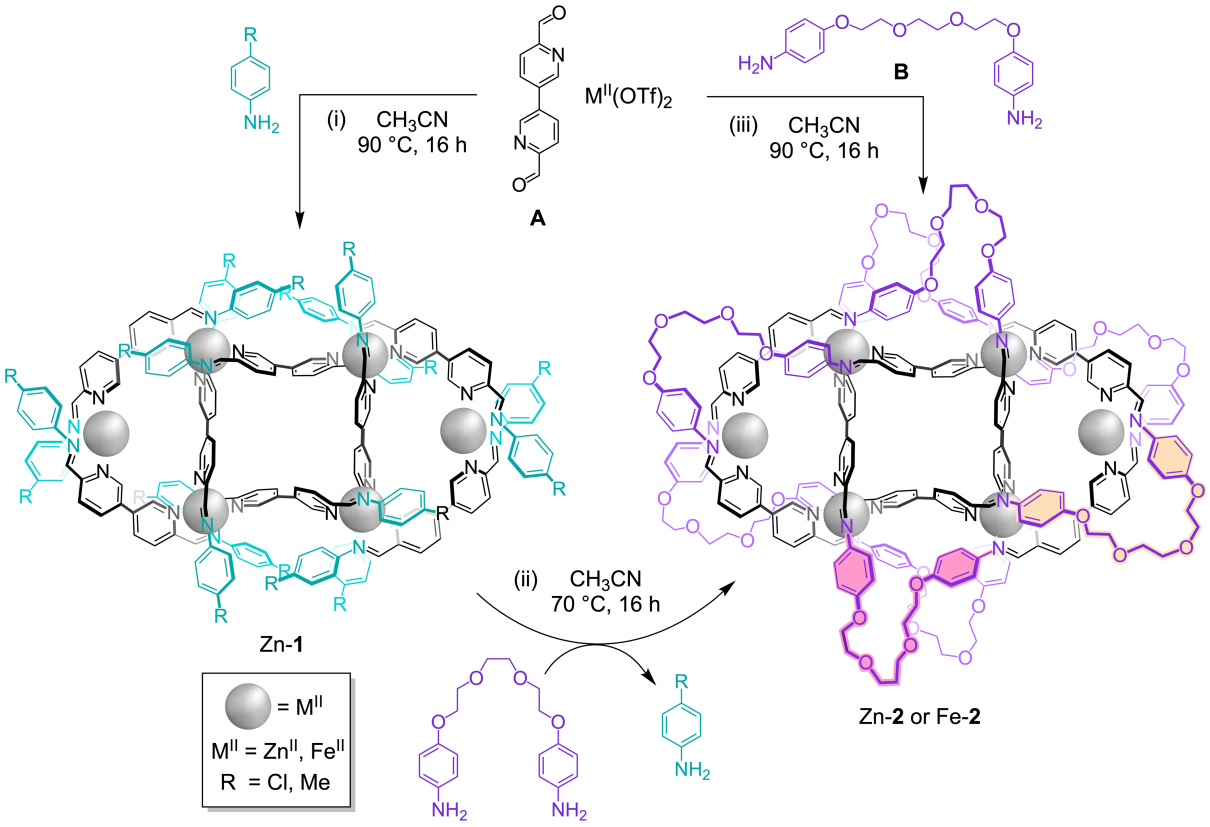

Figure 1 | Synthesis of an eight-crossing molecular knot. (i) Treatment of dialdehyde **A** (8 equiv) with a mono-aniline (16 equiv) and either $Zn(OTf)_2$ or $Fe(OTf)_2$ (6 equiv) led to the formation of the framework of extended circular helicate **1**. Eight-crossing molecular knot **2** formed (ii) *via* aniline exchange from **1**, or (iii) directly from subcomponents **A** and **B** together with the metal template. Exemplars of two types of dianiline linkage are highlighted in pink and orange for clarity. Coordinated triflate anions are omitted.

Within **1**, certain pairs of aniline residues are spatially closer together than others. Noting that each of these proximal anilines were attached to different metal centres, we reasoned that linking them might yield an entangled, topologically complex species. Molecular models suggested that optimal linker length requirements would be met by the triethylene glycol chain of bis-*para*-substituted dianiline **B**.

The reaction of dialdehyde **A** (8 equiv) with dianiline **B** (8 equiv) and zinc(II) trifluoromethanesulfonate (triflate, TfO^-) (6 equiv) in acetonitrile at 90 °C thus produced Zn-**2**, with NMR and ESI-MS analyses consistent with the structure shown in Fig. 1.

Preparing Zn-**2** directly from its subcomponents (Fig. 1, pathway (iii)) led to the formation of a small amount of insoluble precipitate, which we infer to be kinetically-trapped polymeric material. We therefore hypothesised that a stepwise preparation (Fig. 1, pathway (ii)) *via* aniline exchange from extended circular helicate Zn-**1**, incorporating electron-poor 4-chloroaniline, might avoid the formation of these side products.[45] The isolated yield of Zn-**2** was thus found to increase from 72%, for direct assembly, to 92%, using the stepwise approach from the grid Zn-**1** formed from 4-chloroaniline (Supplementary Section 4).

Slow diffusion of diisopropyl ether into an acetonitrile solution of Zn-**2** provided yellow crystals suitable for analysis by single-crystal X-ray diffraction. The solid-state structure unambiguously confirmed that the topology of **2** corresponds to an 8_{19} knot. The organic ligand of the knot weaves a continuous path 240 atoms long around each of the six metal centres, crossing itself eight times. The eight triethylene glycol linkers of dianiline **B** are in four distinct environments (for further details, see Supplementary Section 3), two of which are highlighted in pink and orange in Fig. 1.

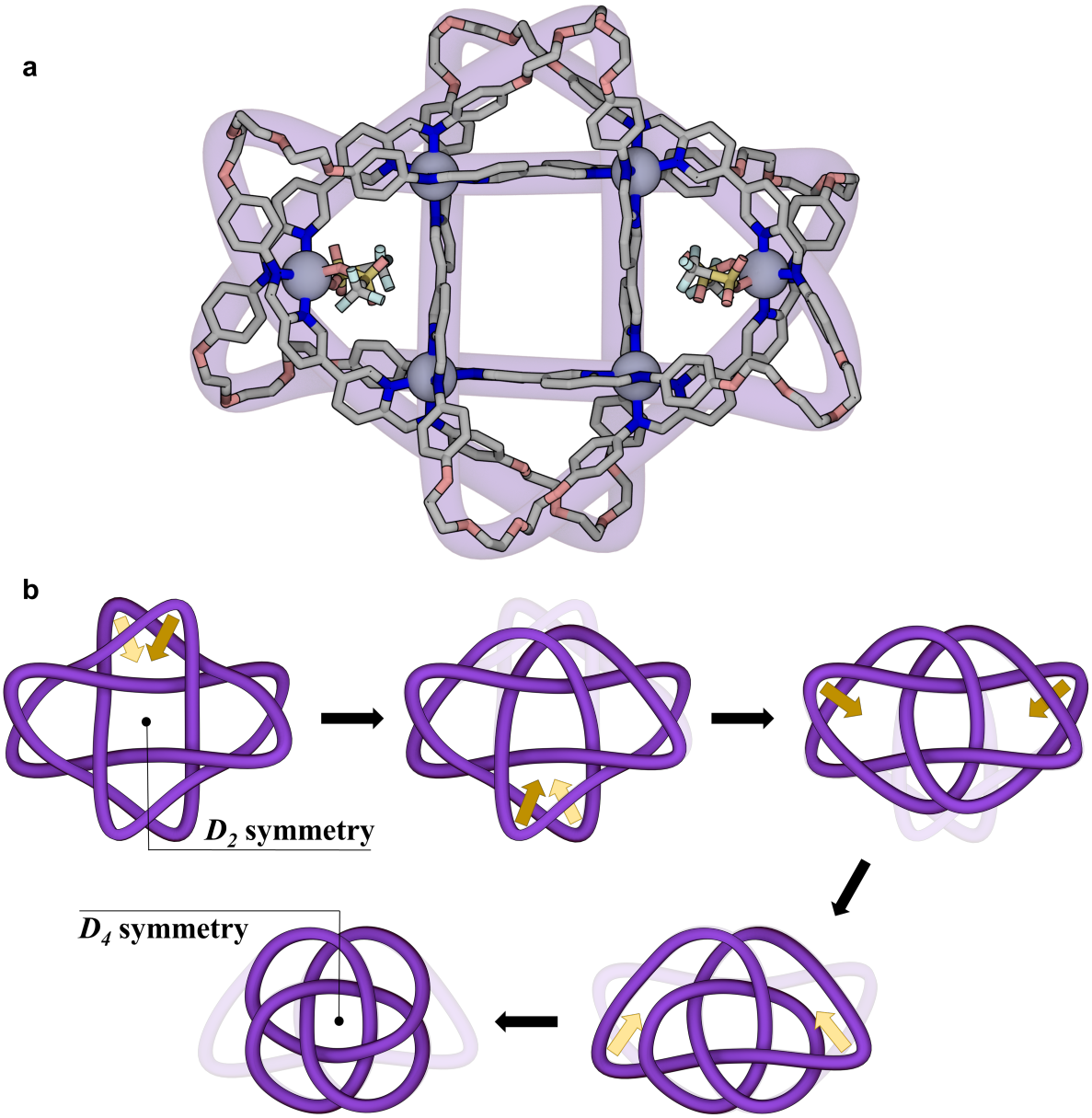

Figure 2 | X-ray crystal structure and topology of molecular knot 2. **a**. X-ray crystal structure of Zn-**2**. Hydrogen atoms, disorder, non-coordinated anions and solvent are omitted for clarity. **b**. Schematic representation of the transformation of D_2–symmetric eight-crossing knot **2** into its topologically equivalent, D_4–symmetric form. Gold and yellow arrows indicate deformation of the knot from its low-symmetry D_2 configuration into its D_4 symmetric form, with gold arrows representing the four Reidemeister type II moves which reduce the number of apparent crossing points from 16 to eight.

The six metal centres of Zn-**2** were found to lie in a common plane. The four central zinc(II) cations are bound by three pyridyl-imine groups, while the peripheral zinc(II) centres are coordinated to two such units, as well as two triflate anions, which together

satisfy an octahedral coordination environment. Both enantiomers of Zn-**2** were observed in the crystal, linked by a centre of inversion.

A similar result was obtained from the reaction of dialdehyde **A** (8 equiv) with dianiline **B** (8 equiv) and iron(II) triflate (6 equiv) in acetonitrile, yielding Fe-**2** (Supplementary Section 5). Fe-**2** was shown to possess the same topology as Zn-**2** by X-ray crystallography (Supplementary Section 12). As in the zinc(II) congener, the octahedral coordination spheres of the two peripheral iron(II) centres of Fe-**2** are each completed by two triflate anions. The low ligand field strength of triflate stabilises the high-spin state of these peripheral iron(II) centres, as reflected in longer Fe-N bond lengths of 2.15 ± 0.04 Å. This high-spin character caused Fe-**2** to exhibit paramagnetism, as seen in its ^{1}H NMR spectrum (Supplementary Section 5). In contrast, the inner iron(II) centres adopted a low-spin state due to the higher ligand field strength of the three pyridyl-imine groups bound to each, with shorter Fe-N bond-lengths of 1.98 ± 0.03 Å.[45]

The Leigh group have reported a topologically-equivalent eight-crossing knot, which possesses D_4 symmetry.[12,46] In contrast, the metallated molecular knots Zn-**2** and Fe-**2** exhibit D_2 symmetry (Supplementary Section 12). Knot **2** appears on first inspection to possess additional crossing points, with 16 seen in total (Fig. 2b). Eight of these crossing points are nugatory: loops may be moved past each other so as to effect their removal, without breaking and re-joining the organic strand (Fig. 2b and Video S1). These manipulations are referred to as Reidemeister moves (Supplementary Section 6), which transform a knot or link into a new representation without altering its topology.[11] Every knot can be deformed using such moves into a configuration which exhibits the minimal number of possible crossing points. Fig. 2b shows four Reidemeister moves which transform **2** into its simplest representation, that of a symmetric torus knot (Fig. 2b, Supplementary Section 6).

Such a symmetric configuration was adopted by fully organic, non-labile eight crossing knot **3**, which was prepared through the reduction and demetallation of Fe-**2** (Fig. 3). Reduction of Fe-**2** with BH_3•THF in an acetonitrile:methanol (5:1, v:v) mixture led to the transformation of the labile imine linkages holding the parent structure together into fixed secondary amines,[47] thus leading to the formation of the fully organic knot **3**,

as confirmed by mass spectrometry (Supplementary Section 7). In contrast to the 24 aromatic ^{1}H NMR resonances observed for Zn-**2** (Fig. 3b), only five were observed for **3** (Fig. 3c). The constitutionally equivalent sections of knot **3** thus reside in magnetically equivalent environments.[12,46] Variable temperature NMR experiments showed this equivalence to persist over a temperature range of 25 °C – −50 °C (Supplementary Section 7).

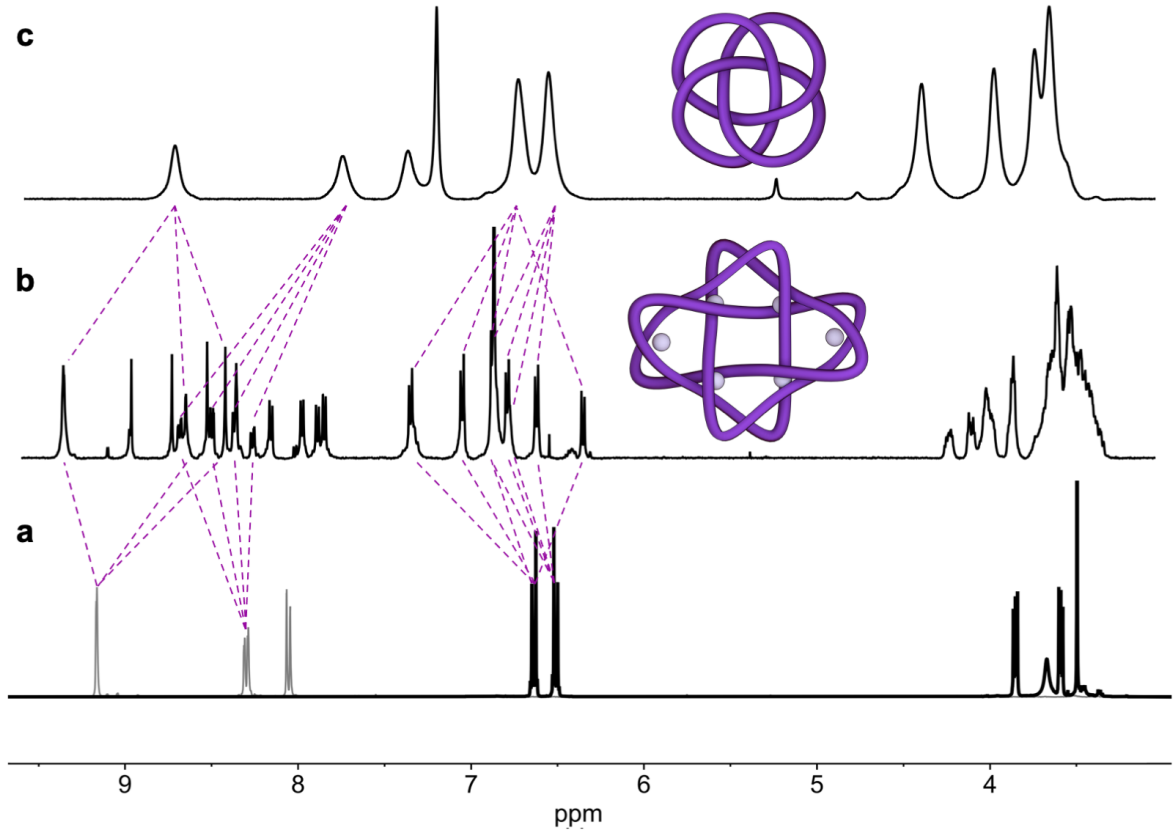

Figure 3 | ^{1}H NMR spectra of knots Zn-2 and 3. Partial ^{1}H NMR spectra of **a**. superimposed spectra of dialdehyde **A** (grey) and dianiline **B** (black) with no transition metal salt added (500 MHz, 298 K, CD_3CN), **b**. metallated molecular knot Zn-**2** (500 MHz, 298 K, CD_3CN) and **c**. demetallated and reduced, purely-organic, knot **3** synthesised from Fe-**2** (500 MHz, 298 K, $CDCl_3$).

The 8_{19} knot is inherently topologically chiral, a property resulting from its spatial connectivity. When achiral subcomponents were incorporated, the expected racemic mixture of the two knot enantiomers was obtained. These topological enantiomers could be distinguished by adding the tetrabutylammonium salt of Lacour's Δ-

TRISPHAT to Zn-**2**,[48] which led to a separate ^{1}H NMR spectrum for each enantiomer (Supplementary Section 8).

We hypothesised that incorporating remote stereocentres into the dianiline subcomponent would lead to the formation of a knot having a single topological handedness.[25,49] We therefore synthesised enantiopure dianilines **C**-(1*R*,2*R*) and **C**-(1*S*,2*S*) (Supplementary Section 9). These dianilines provide a similar-length chain to that of dianiline **B**.

The reaction of dialdehyde **A** (8 equiv) with dianiline **C**-(1*R*,2*R*) (8 equiv) and iron(II) triflate (6 equiv) resulted in the formation of molecular knot Fe-**4**-(1*R*,2*R*), as evidenced by ESI- low and high resolution mass spectrometry (Figures S36 and S37). The paramagnetic ^{1}H NMR spectrum of Fe-**4**-(1*R*,2*R*) (Figure S34) was similar to that of Fe-**2**, and to that obtained in the case of Fe-**4**-(1*S*,2*S*), formed from **C**-(1*S*,2*S*) (Supplementary Section 10, Figure S35).

Circular dichroism (CD) spectroscopy was used to gauge the stereoselectivity of the formation of knots Fe-**4**-(1*R*,2*R*) and Fe-**4**-(1*S*,2*S*). CD spectra show bands of equal and opposite intensity for Fe-**4**-(1*R*,2*R*) and Fe-**4**-(1*S*,2*S*). Furthermore, intense bisignate MLCT bands centred at 581 nm were observed in the CD for each (Fig. 4b). Equal and opposite signals centred at 581 nm were recorded for Fe-**4**-(1*R*,2*R*) and Fe-**4**-(1*S*,2*S*). This confirms the presence of non-racemic stereogenic metal centres, and indicates that Fe-**4**-(1*R*,2*R*) contains Δ iron centres, and Fe-**4**-(1*S*,2*S*) Λ.[50,51,52] Only one set of peaks were apparent by ^{1}H NMR spectroscopy (Supplementary Section 10). These observations indicated that the stereochemical information of the chiral cyclohexane residues was effectively communicated to the metal centres of the molecular knot during self-assembly, thereby resulting in the favoured formation of one knot stereoisomer. Stereochemical information transmission thus occurred efficiently over a path of at least 10 atoms in order to dictate the handedness of the metal centres, with the 16 stereogenic units acting in concert to exert strong control.

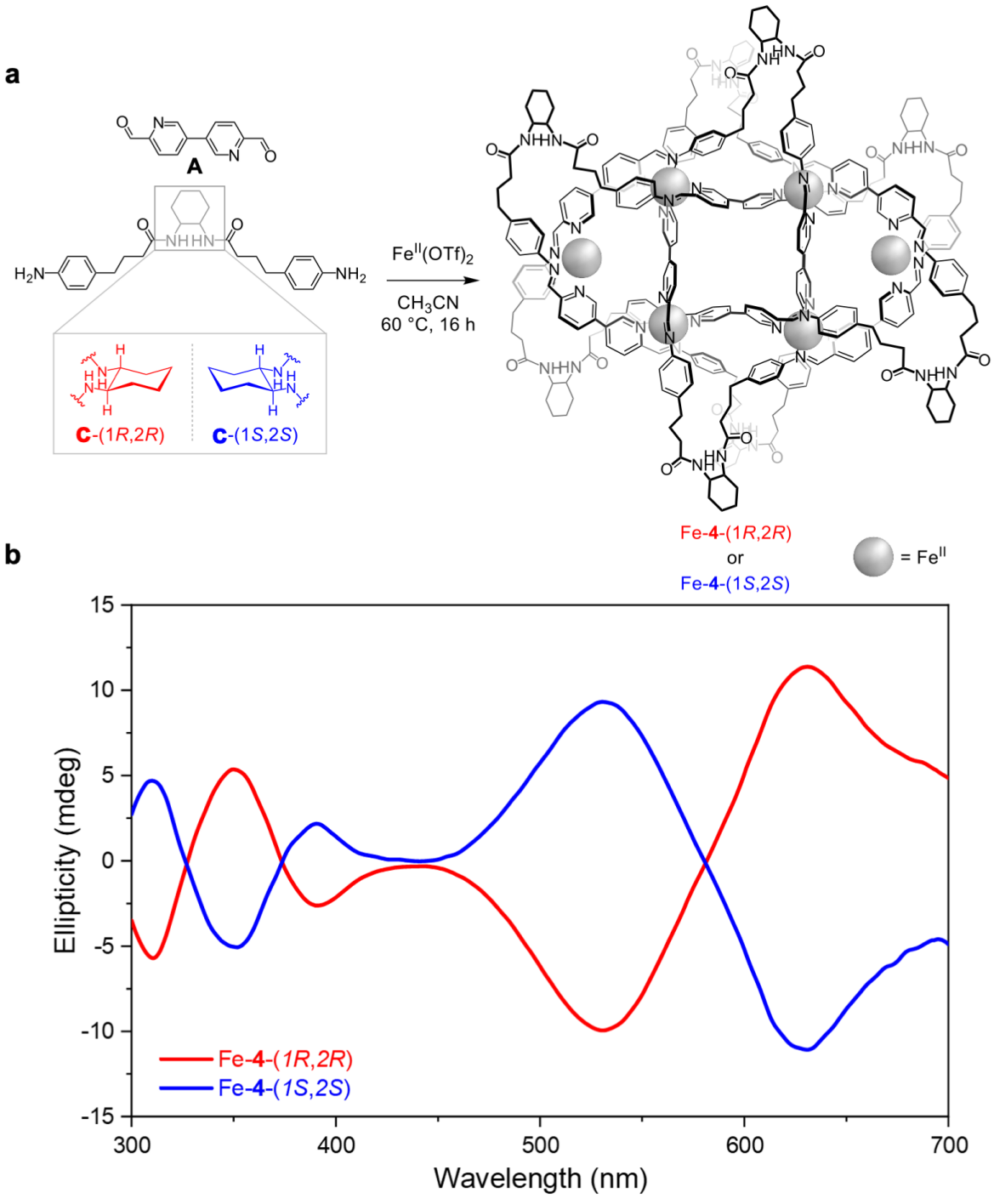

Figure 4 | Diastereoselective self-assembly of an eight-crossing knot. **a**. Treatment of subcomponent **A** (8 equiv) with iron(II) triflate (6 equiv) and either **C**-(1*R*,2*R*) or **C**-(1*S*,2*S*) (8 equiv) led to the stereoselective synthesis of eight crossing knots Fe-**4**-(1*R*,2*R*) and Fe-**4**-(1*S*,2*S*), respectively. **b**. CD spectra of Fe-**4**-(1*R*,2*R*) and Fe-**4**-(1*S*,2*S*) at 298 K in CH_3CN at the same concentration (10 μM).

Zinc(II)-templated molecular knots Zn-**4**-(1*R*,2*R*) and Zn-**4**-(1*S*,2*S*) were prepared by an analogous self-assembly process (Supplementary Section 11). ^{1}H NMR spectroscopy showed formation of one major diastereomer in each case (Supplementary Section 11). CD spectroscopy again revealed strong bands of equal and opposite intensity (Figure S49).

The successful synthesis and reductive demetallation of a metal-organic eight crossing point knot *via* a simple, one-pot, and high-yielding procedure highlights the power of subcomponent self-assembly in the formation of entangled species with complex topology.[13,45,53] The ability to control the shape and geometric configuration of these entanglements, as well as their topological chirality, will enhance our ability to probe the fundamental effects of such entanglements on the molecular level. This will inform the development of nanoscale woven materials, molecular devices and future innovations in the field.

Methods

Preparation of [Zn-2](OTf)$_{12}$. 6,6´-Diformyl-3,3´-bipyridine **A** (3.56 mg, 16.8 μmol, 8 equiv), 4,4'-(((ethane-1,2-diylbis(oxy))bis(ethane-2,1-diyl))bis(oxy))dianiline **B** (5.60 mg, 16.8 μmol, 8 equiv) and $Zn(OTf)_2$ (4.44 mg, 12.2 μmol, 6 equiv) were added to a small Schlenk flask (total volume 4 mL). CH_3CN (1 mL) was added along with a Teflon-coated magnetic stir-bar. The sealed Schlenk flask was sonicated for 10 minutes at 70 °C and left to stir at 90 °C for 18 hours. The light-yellow reaction mixture was allowed to cool to room temperature and was then filtered through a glass fibre filter (0.7 μm pore size). Addition of diisopropyl ether (2 mL) resulted in the precipitation of a yellow solid. The suspension was then centrifuged (10 min, 3000 RPM), the eluent decanted. Further diisopropyl ether (2 mL) was added, the powder was resuspended by sonication and then centrifuged. Again, the eluent was decanted. The residue was then dried *in vacuo* to afford the solid product as a light-yellow powder (9.9 mg, 72%). ^{1}H NMR (500 MHz, 298 K, CD_3CN) δ: 9.42 (s, 4H), 9.41 (s, 4H), 9.02 (s, 4H), 8.79 (s, 4H), 8.74 (dd, J = 8.4, 2.2 Hz, 4H), 8.71 (d, J = 2.1 Hz, 4H), 8.58 (s, 4H), 8.56 (dd, J = 8.0, 2.0 Hz, 4H), 8.48 (s, 4H), 8.43 (dd, J = 8.0, 2.3 Hz, 4H), 8.42 (s, 4H), 8.32 (dd, J

= 8.4, 2.4 Hz, 4H), 8.22 (d, J = 8.3 Hz, 4H), 8.04 (d, J = 7.9 Hz, 4H), 7.95 (d, J = 8.3 Hz, 4H), 7.91 (d, J = 8.0 Hz, 4H), 7.41 (d, J = 8.7 Hz, 4H), 7.11 (d, J = 8.9 Hz, 8H), 6.94 (d, 8H, overlapped), 6.93 (d, overlapped, 8H), 6.93 (d, overlapped, 8H), 6.85 (d, J = 8.8 Hz, 4H), 6.68 (d, J = 8.9 Hz, 4H), 6.41 (d, J = 8.8 Hz, 4H), 4.32–3.40 (H, m, aliphatic, 96H). ^{13}C NMR (125 MHz, 298 K, CD3CN) δ: 164.9, 162.0, 161.2, 161.1, 160.5, 160.3, 160.1, 157.3, 150.4, 150.0, 149.3, 149.3, 147.9, 147.9, 147.6, 147.4, 146.8, 142.6, 141.9, 141.9, 140.4, 139.7, 139.4, 139.2, 138.9, 137.4, 137.3, 137.2, 136.7, 135.6, 131.2, 130.9, 130.9, 128.9, 125.7, 124.5, 124.0, 123.7, 118.2, 116.6, 116.1, 115.8, 73.3, 72.0, 71.4, 71.3, 71.2, 71.0 70.3, 70.1, 70.1, 69.9, 69.5, 69.2, 68.8, 68.8, 68.7, 62.0.

Preparation of [Zn-4](OTf)$_{12}$. 6,6´-Diformyl-3,3´-bipyridine **A** (14.2 mg, 67.0 mmol, 8 equiv), **C**-(1*R*,2*R*) (29.5 mg, 66.1 mmol, 8 equiv) and Zn(OTf)$_2$ (18.4 mg, 49.0 mmol, 6 equiv) were added to a small Schlenk flask (total volume 25 mL). CH_3CN (8 mL) was added along with a Teflon-coated magnetic stir-bar. The sealed Schlenk flask was sonicated for 10 minutes at 70 °C and left to stir at 90 °C for 18 hours. The light-yellow reaction mixture was allowed to cool to room temperature and was then filtered through a glass fibre filter (0. 7 μm pore size). The acetonitrile solution was concentrated under a stream of N_2 to a volume of 2 mL. Addition of diisopropyl ether (6 mL) resulted in the precipitation of a yellow solid. The suspension was then centrifuged (10 min, 3000 RPM), the eluent decanted. Further diisopropyl ether (2 mL) was added, the powder was resuspended by sonication and then centrifuged. Again, the eluent was decanted. The residue was then dried *in vacuo* to afford the solid product as a fine light-yellow powder (44 mg, 73%). ^{1}H NMR (500 MHz, 298 K, CD_3CN) δ: 9.48 (d, J = 2.1 Hz, 4H), 9.40 (d, J = 2.1 Hz, 4H), 9.11 (s, 4H), 8.93 (s, 4H), 8.75 (s, 4H), 8.72 (dd, J = 7.9, 2.1 Hz, 4H), 8.70 (dd, J = 7.9, 2.1 Hz, 4H), 8.57 (s, 4H), 8.49 (s, 4H), 8.44 (dd, J = 8.0, 2.1 Hz, 4H), 8.33 (dd, J = 8.3, 2.2 Hz, 4H), 8.28 (d, J = 8.3 Hz, 4H), 8.11 (d, J = 2.2 Hz, 4H), 8.05 (d, J = 2.2 Hz, 4H), 8.02 (d, J = 2.2 Hz, 4H), 7.86 (d, J = 8.0 Hz, 4H), 7.76 (d, J = 8.6 Hz, 4H, amide NH), 7.36 (d, J = 8.3 Hz, 8H), 7.22 (d, J = 8.2 Hz, 8H), 7.12 (d, J = 8.2 Hz, 8H), 7.10 (d, J = 8.4 Hz, 8H), 6.96 (d, J = 8.5 Hz, 8H), 6.84 (d, J = 8.0 Hz, 8H), 6.79 (d, J = 6.5 Hz, 4H, amide NH), 6.69 (d, J = 8.7 Hz, 8H), 6.64 (d, J = 6.7 Hz, 4H, amide NH), 6.37 (d, J = 8.1 Hz, 8H, amide NH), 6.09 (d, J = 8.3 Hz, 8H), 3.86–3.76 (4H, m), 3.65–3.53 (16H, m), 2.92–2.83 (4H, m),

2.66–2.39 (32H, m), 2.37–2.29 (4H, m), 2.37–2.29 (4H, m), 1.85–1.62 (56H, m), 1.42–1.14 (56H, m). ^{13}C NMR (125 MHz, 298 K, CD_3CN) δ: 174.0, 173.8, 173.5, 173.2, 172.8, 165.5, 163.2, 161.8, 158.3, 150.2, 149.9, 148.8, 147.6, 147.5, 147.1, 147.0, 146.7, 146.0, 145.5, 144.8, 144.5, 144.1, 143.9, 143.9, 143.7, 142.8, 142.7, 142.5, 142.0, 140.7, 138.9, 137.5, 136.8, 136.1, 131.7, 131.6, 131.3, 131.2, 130.7, 130.4, 130.1, 129.9, 128.9, 123.9, 122.5, 122.3, 122.2, 55.4, 54.2, 53.7, 52.1, 37.6, 36.8, 36.5, 36.3, 36.2, 35.7, 35.5, 35.0, 34.4, 34.1, 33.7, 33.4, 33.1, 32.9, 32.7, 28.8, 28.7, 28.5, 26.6, 26.0, 25.7, 25.6, 25.5. Not all of the expected peaks in the aliphatic region of the 13C NMR spectrum could not be resolved due to overlapping signals.

Complete assignment of both [Zn-**2**](OTf)$_{12}$ and [Zn-**4**](OTf)$_{12}$ are available in the Supplementary Information. Details for the synthesis of both [Fe-**2**](OTf)$_{12}$ and [Fe-**4**](OTf)$_{12}$ are available in the Supplementary Information.

Preparation of 3. To a stirred solution of [Fe-**2**](OTf)$_{12}$ (62 mg, 10 μmol, 1 equiv) in MeCN/MeOH (5/1, v/v, 12 mL total volume) at room temperature was added BH_3•THF (1 M, 480 μL, 480 μmol, 3 equiv/imine). The mixture was stirred for 10 minutes as the colour of the solution changed from deep green to dark brown. CH_2Cl_2 (10 mL) and ethylenediamine (18 μL, 0.27 mmol, 4.5 equiv/Fe^{II}) were then added and the mixture was stirred for 10 minutes. The resulting suspension was poured in 30 mL H_2O and the mixture was extracted with 10 × 5 mL CH_2Cl_2 (note: the emulsions were broken mechanically). The combined organic layers were filtered on cotton covered with sand, then solvents were removed *in vacuo*. The residue was dissolved in CH_2Cl_2, filtered over Celite and dried *in vacuo* affording the reduced and demetallated knot **3** (25.4 mg, 6.19 μmol, 62%).

References

1. M. Huurre in *9000 vuotta Suomen esihistoriaa*, Otava, Helsinki, p. 18 (1979).
2. Sułkowska, J. I., Rawdon, E. J., Millett, K. C., Onuchic, J. N. & Stasiak, A. Conservation of complex knotting and slipknotting patterns in proteins. *Proc. Natl. Acad. Sci. USA* **109**, E1715–E1723 (2012).

3. Lui, L. F., Lui, C.-C. & Alberts, B. M. Type II DNA Topoisomerases: Enzymes that can unknot a topologically knotted DNA molecules *via* a reversible double-strand break. *Cell* **19**, 687–707 (1980).
4. Frank-Kamenetskii, M. D., Lukashin, A. V. & Vologodskii, A. V. Statistical mechanics and topology of polymer chains. *Nature* **258**, 398–402 (1975).
5. Jones, C. D., Simmons, H. T. D., Horner, K. E., Liu, K., Thompson, R. L. & Steed, J. W. Braiding, branching and chiral amplification of nanofibres in supramolecular gels. *Nat. Chem.* **11**, 375–381 (2019).
6. Saitta, A. M., Soper, P. D., Wasserman, E. & Klein, M. L. Influence of a knot on the strength of a polymer strand. *Nature* **399**, 46–48 (1999).
7. Wikoff, W. R., Liljas, L., Duda, R. L., Tsuruta, H., Hendrix, R. W. & Johnson, J. E. Topologically linked protein rings in the bacteriophage HK97 capsid. *Science* **289**, 2129–2133 (2000).
8. Liu, Y., Ma, Y., Zhao, Y., Sun, X., Gándara, F., Furukawa, H., Liu, Z., Zhu, H., Zhu, C., Suenaga, K., Oleynikov, P., Alshammari, A. S., Zhang, X., Terasaki, O. & Yaghi, O. M. Weaving of organic threads into a crystalline covalent organic framework. *Science* **351**, 365–369 (2016).
9. Wu, Q., Rauscher, P. M., Lang, X., Wojtecki, R. J., de Pablo, J. J., Hore, M. J. A. & Rowan, S. J. Poly[n]catenanes: Synthesis of molecular interlocked chains. *Science* **358**, 1434–1439 (2017).
10. Dietrich-Buchecker, C. O. & Sauvage, J.-P. A synthetic molecular trefoil knot. *Angew. Chem. Int. Ed.* **28**, 189–192 (1989).
11. Fielden, S. D. P., Leigh, D. A. & Woltering, S. L. Molecular knots. *Angew. Chem. Int. Ed*. **56**, 11166–11194 (2017).
12. Danon, J. J., Krüger, A., Leigh, D. A., Lemonnier, J.-P., Stephens, A. J., Vitorica-Yrezabal I. J. & Woltering. S. L. Braiding a molecular knot with eight crossings. *Science* **355**, 159–162 (2017).
13. Ayme, J.-P., Beves, J. A., Leigh, D. A., McBurney, R. T., Rissanen, K. & Schultz, D. A synthetic molecular pentafoil knot. *Nat. Chem.* **4**, 15–20 (2012).
14. Ponnuswamy, N., Cougnon, F. B. L., Clough, J. M., Pantoş, G. D. & Sanders, J. K. M. Discovery of an organic trefoil knot. *Science* **338**, 783–785 (2012).

15. Kim, D. H., Jihun, N. S., Kim, O. E-H., Jung, J., Kim, H. & Chi, K. W. Coordination-driven self-assembly of a molecular knot comprising sixteen crossings. *Angew. Chem. Int. Ed*. **57**, 5669–5673 (2017).
16. Inomata, Y., Sawada, T. & Fujita, M. Metal-peptide torus knots from flexible short peptides. *Chem* **6**, 294–303 (2020).
17. Sawada, T., Inomata, Y., Shimokawa, K. & Fujita, M. A metal-peptide capsule by multiple ring threading. *Nat. Commun.* **10**, 5687 (2019).
18. Sawada, T., Saito, A., Tamiya, K., Shimokawa, K., Hisada, Y., Fujita, M. Metal-peptide rings form highly entangled topologically inequivalent frameworks with the same ring- and crossing-numbers. *Nat. Commun.* **10**, 921 (2019).
19. Marcos, V., Stephens, A. J., Jaramillo-Garcia, J., Nussbaumer, A. L., Woltering, S. L., Valero, A., Lemonnier, J.-F., Vitorica-Yrezabal, I. J. & Leigh, D. A. Allosteric initiation and regulation of catalysis with a molecular knot. *Science* **352**, 1555–1559 (2016).
20. Leigh, D. A., Pirvu, L., Schaufelberger, F., Tetlow, D. J. & Zhang, L. Securing a supramolecular architecture by tying a stopper knot. *Angew. Chem. Int. Ed.* **57**, 10484–10488 (2018).
21. Adams, H., Ashworth, E., Breault, G. A., Guo, J., Hunter, C. A. & Mayers, P. C. Knot tied around an octahedral metal centre. *Nature* **411**, 763 (2001).
22. Cougnon, F. B. L., Caprice, K., Pupier, M., & Bauza, A., Frontera, A. A strategy to synthesize molecular knots and links using the hydrophobic effect. *J. Am. Chem. Soc*. **140**, 12442–12450 (2018).
23. Feigel, M., Ladberg, R., Engels, S., Herbst-Irmer, R. & Fröhlich, R. A trefoil knot made of amino acids and steroids. *Angew. Chem. Int. Ed.* **45**, 5698–5702 (2006).
24. Guo, J., Mayers, P. C., Breault, G. A. & Hunter, C. A. Synthesis of a molecular trefoil knot by folding and closing on an octahedral coordination template. *Nat. Chem*. **2**, 218–222 (2010).
25. Barran, P. E., Cole, H. L., Goldup, S. M., Leigh, D. A., McGonigal, P. R., Symes, M. D., Wu, J. Y. & Zengerle, M. Active-metal template synthesis of a molecular trefoil knot. *Angew. Chem. Int. Ed*. **50**, 12280–12284 (2011).

26. Prakasam, T., Lusi, M., Elhabiri, M., Platas-Iglesias, C., Olsen, J.-C., Asfari, Z., Cianferani-Sanglier, S., Debaene, F., Charbonniere, L. J. & Trabolsi, A. Simultaneous self-assembly of a [2]catenane, a trefoil knot, and a solomon link from a simple pair of ligands. *Angew. Chem. Int. Ed*. **52**, 9956–9960 (2013).
27. Ayme, J.-F., Gil-Ramírez, G., Leigh, D. A., Lemonnier, J.-F., Markevicius, A., Muryn, C. A. & Zhang, G. Lanthanide template synthesis of a molecular trefoil knot. *J. Am. Chem. Soc.* **136**, 13142–13145 (2014).
28. Leigh, D. A., Pirvu L. & Schaufelberger, F. Stereoselective synthesis of molecular square and granny knots. *J. Am. Chem. Soc*. **141**, 6054–6059 (2019).
29. Dietrich-Buchecker, C. & Rapenne, G. Efficient synthesis of a molecular knot by copper(I)-induced formation of the precursor followed by ruthenium(II)-catalysed ring closing metathesis. *Chem. Commun*. 2053–2054 (1997).
30. Ponnuswamy, N., Cougnon, F. B. L., Pantos, G. D. & Sanders, J. K. M. Homochiral and *meso* figure eight knots and a Solomon link. *J. Am. Chem. Soc*. **136**, 8243–8251 (2014).
31. Zhang, L., Stephens, A. J., Nussbaumer, A. L., Lemonnier, J.-F., Jurcek, P., Vitorica-Yrezabal, I. J. & Leigh, D. A. Stereoselective synthesis of a composite knot with nine crossings. *Nat. Chem*. **10**, 1083–1088 (2018).
32. Beves, J. E., Danon, J. J., Leigh, D. A., Lemonnier, J.-F. & Vitorica-Yrezabal, I. J. A Solomon link through an interwoven molecular grid. *Angew. Chem. Int. Ed*. **54**, 7555–7559 (2015).
33. Ayme, J.-F., Beves, J. E, Campbell, C. J. & Leigh, D. A. The self-sorting behavior of circular helicates and molecular knots and links. *Angew. Chem. Int. Ed*. **53**, 7823–7827 (2014).
34. Gil-Ramírez, G., Hoekman, S., Kitching, M. O., Leigh, D. A., Vitorica-Yrezabal, I. J. & Zhang, G. Tying a molecular overhand knot of single handedness and asymmetric catalysis with the corresponding pseudo-D_3-symmetric trefoil knot. *J. Am. Chem. Soc*. **138**, 13159–13162 (2016).
35. Ayme, J.-F., Beves, J. E., Campbell, C. J., Gil-Ramírez, G., Leigh, D. A. & Stephens, A. J. Strong and selective anion binding within the central cavity of molecular knots and links. *J. Am. Chem. Soc*. **137**, 9812–9815 (2015).

36. Gardner, M. *The Ambidextrous Universe: Symmetry and Asymmetry, From Mirror Reflections to Superstrips* 3rd ed. (W. H. Freeman and Company, New York, 1990).
37. Brandt, J., Salerno, F. & Fuchter, M. The added value of small-molecule chirality in technological applications. *Nat. Rev. Chem.* **1**, 0045 (2017).
38. Chirality in Supramolecular Assemblies: Causes and Consequences. Ed.: Keene, F. R. Wiley, Chichester (2016).
39. Maynard, J. R. J. & Goldup, S. M. Strategies for the synthesis of enantiopure mechanically chiral molecules. *Chem* **6**, 1914–1932.
40. Perret-Aebi, L-E., von Zelewsky, A., Dietrich-Buchecker, C. & Sauvage, J.-P. Stereoselective synthesis of a topologically chiral molecule: the trefoil knot. *Angew. Chem. Int. Ed*. **43**, 4482–4485 (2004).
41. Zhang, G., Gil-Ramírez, G., Markevicius, A., Browne, C., Vitorica-Yrezabal, I. J. & Leigh, D. A. Lanthanide template synthesis of trefoil knots of single handedness. *J. Am. Chem. Soc.* **137**, 10437–10442 (2015).
42. Riddell, I. A. *et al.* Anion-induced reconstitution of a self-assembling system to express a chloride-binding $Co_{10}L_{15}$ pentagonal prism. *Nat. Chem.* **4**, 751–756 (2012).
43. Riddell, I. A. *et al.* Five discrete multinuclear metal-organic assemblies from one ligand: deciphering the effects of different templates. *J. Am. Chem. Soc*. **135**, 2723–2733 (2013).
44. Riddell, I. A. *et al.* Cation- and anion-exchanges induce multiple distinct rearrangements within metallosupramolecular architectures. *J. Am. Chem. Soc*. **136**, 9491–9498 (2014).
45. Wood, C. S., Ronson, T. K., Belenguer, A. M., Holstein, J. J. & Nitschke, J. R. Two-stage directed self-assembly of a cyclic [3]catenane. *Nat. Chem.* **7**, 354–358 (2015).
46. Zhang, L., Lemonnier, J.-F., Acocella, A., Calvaresi, M., Zerbetto. F. & Leigh, D. A. Effects of knot tightness at the molecular level. *Proc. Natl. Acad. Sci. USA*. **116**, 2452–2457 (2019).

47. Lavendomme, R., Ronson T. K. & Nitschke, J. R. Metal and organic templates together control the size of covalent macrocycles and cages. *J. Am. Chem. Soc*. **141**, 12147–12158 (2019).
48. Favarger, F., Goujon-Ginglinger, C., Monchaud, D. & Lacour, J. Large-scale synthesis and resolution of TRISPHAT [Tris(tetrachlorobenzenediolato) phosphate(V)] anion. *J. Org. Chem.* **69**, 8521–8524 (2004).
49. Greenfield, J. L. *et al*. Unraveling mechanisms of chiral induction in double-helical metallopolymers. *J. Am. Chem. Soc*. **140**, 10344–10353 (2018).
50. Howson, S. E., Allan, L. E. N., Chmel, N. P., Clarkson, G. J., van Gorkum, R. & Scott, P. Self-assembling optically pure $Fe(A\text{-}B)_3$ chelates. *Chem. Commun.* **13**, 1727–1729 (2009).
51. Howson, S. E., Allan, L. E. N., Chmel, N. P., Clarkson, G. J., Deeth, R. J., Faulkner, A. D., Simpson, D. H. & Scott, P. Origins of stereoselectivity in optically pure phenylethaniminopyridine *tris*-chelates $M(NN')_3^{n+}$ (M = Mn, Fe, Co, Ni and Zn). *Dalton Trans.* **40**, 10416–10433 (2011).
52. Knof, U. & von Zelewsky, A. Predetermined chirality at metal centers. *Angew. Chem. Int. Ed.* **38**, 302–322 (1999).
53. Chichak, K. S., Cantrill, S. J., Pease, A. R., Chiu, S.-H. Cave, G. W. V., Atwood, J. L. & Stoddart, J. F. Molecular borromean rings. *Science* **304**, 1308–1312 (2004).

Acknowledgements

This work was supported by the European Research Council (695009), the UK Engineering and Physical Sciences Research Council (EPSRC EP/P027067/1) and a Marie Curie fellowship for J.P.C. (ITN-2010-264645). C.T.M. thanks the Leverhulme and Isaac Newton Trusts, and Sidney Sussex College, Cambridge, for Fellowship support. The authors thank the Department of Chemistry NMR facility, University of Cambridge for performing some NMR experiments, the EPSRC UK National Mass Spectrometry Facility at Swansea University and the Department of Chemistry Mass Spectrometry Facility, University of Cambridge, for carrying out high resolution mass

spectrometry, and Diamond Light Source (UK) for synchrotron beamtime on I19 (MT15768).

Author Contributions

JPC and JRN conceived the project. JPC, CTM, JLG and RL performed the experiments and analysed the data. TKR collected the X-ray data and refined the structures. All authors discussed the results and edited the manuscript.

Additional Information

Crystallographic data for the structures reported in this paper have been deposited at the Cambridge Crystallographic Data Centre, under the deposition numbers 2000486 (Zn-**2**) and 2000487 (Fe-**2**). Copies of these data can be obtained free of charge via www.ccdc.cam.ac.uk/data_request/cif. Reprints and permissions information is available at www.nature.com/reprints. The authors declare no competing financial interests. Supplementary information and chemical compound information accompany this paper at www.nature.com/naturechemistry. Correspondence and requests for materials should be addressed to JRN.

Competing financial interests

The authors declare no competing financial interests